

Investigating the (Poly)radicaloid Nature of Real-World Organic Compounds with DFT-Based Methods

Giovanna Salvitti, Fabrizia Negri, Ángel José Pérez-Jiménez, Emilio San-Fabián, David Casanova, and Juan Carlos Sancho-García

J. Phys. Chem. A, **Just Accepted Manuscript** • DOI: 10.1021/acs.jpca.0c01239 • Publication Date (Web): 10 Apr 2020

Downloaded from pubs.acs.org on April 14, 2020

Just Accepted

“Just Accepted” manuscripts have been peer-reviewed and accepted for publication. They are posted online prior to technical editing, formatting for publication and author proofing. The American Chemical Society provides “Just Accepted” as a service to the research community to expedite the dissemination of scientific material as soon as possible after acceptance. “Just Accepted” manuscripts appear in full in PDF format accompanied by an HTML abstract. “Just Accepted” manuscripts have been fully peer reviewed, but should not be considered the official version of record. They are citable by the Digital Object Identifier (DOI®). “Just Accepted” is an optional service offered to authors. Therefore, the “Just Accepted” Web site may not include all articles that will be published in the journal. After a manuscript is technically edited and formatted, it will be removed from the “Just Accepted” Web site and published as an ASAP article. Note that technical editing may introduce minor changes to the manuscript text and/or graphics which could affect content, and all legal disclaimers and ethical guidelines that apply to the journal pertain. ACS cannot be held responsible for errors or consequences arising from the use of information contained in these “Just Accepted” manuscripts.

1
2
3
4
5
6
7
8
9
10
11
12
13
14
15
16
17
18
19
20
21
22
23
24
25
26
27
28
29
30
31
32
33
34
35
36
37
38
39
40
41
42
43
44
45
46
47
48
49
50
51
52
53
54
55
56
57
58
59
60

Investigating the (poly)radicaloid nature of real-world organic compounds with DFT-based methods

G. Salvitti^{a,b}, F. Negri^{b,c},
A.J. Pérez-Jiménez^a, E. San-Fabián^a,
D. Casanova^{d,e}, and J. C. Sancho-García^{a*}

^a Department of Physical Chemistry,
University of Alicante,
E-03080 Alicante, Spain

^b Dipartimento di Chimica “Giacomo Ciamician”,
Università di Bologna,
IT-40126 Bologna, Italy

^c INSTM UdR Bologna, Italy

^d Donostia International Physics Center (DIPC),
E-20018 Donostia, Spain

^e IKERBASQUE,
Basque Foundation for Science,
E-48013 Bilbao, Spain

April 9, 2020

*E-mail: jc.sancho@ua.es

Abstract

Recent advances in the synthesis of stable organic (open-shell) polyradicaloids have opened their application as active compounds for emerging technologies. These systems typically exhibit small energy differences between states with different spin multiplicities, which are intrinsically difficult to calculate by theoretical methods. We thus apply here some DFT-based variants (FT-DFT, SF-DFT, and SF-TDDFT) on a test set of large and real-world molecules, as test systems for which such energy differences are experimentally available, also comparing systematically with RAS-SF results to infer if shortcomings of previous DFT applications are corrected. Additionally, we explore the spin-spin contribution to the ZFS tensor, of high interest for EPR spectroscopy, and derive the spatial extent of the corresponding (photoexcited) triplet state.

Key words: organic (poly)radicals, low- and high-spin states, finite-temperature DFT, spin-flip (TD)DFT, ZFS tensor.

Introduction

Studying the (poly)radical character of organic molecules is a long-standing field of research due to the many envisioned applications of these compounds.^{1,2} Recent experimental developments, in ultrahigh-vacuum surfaces or using non-standard synthetic routes, have propelled the synthesis of highly challenging species including classically studied carbon-rich radicals³ like triangulenes,⁴ graphene nanoribbons with zigzag edges,^{5,6} kekulenes,⁷ long acenes,^{8,9} cyclic nanobelts,^{10,11} etc. All these systems share a complicated electronic structure, with (near-)degenerated orbitals lying within the gap between occupied and virtual ones, leading to small exchange interactions and thus close in energy low- (e.g. singlet or doublet) and high-spin (e.g. triplet or quartet) many-body states.¹² Furthermore, C-based magnetism is gaining attention for nanographene fragments since long time ago,¹³ and it has been recently demonstrated for well-defined geometrical C-based structures, like those arising from planar conjugated hydrocarbons, how to anticipate the spin multiplicity and energy ordering of the corresponding states,¹⁴ thus complementing the Ovchinnikov's rule¹⁵ and the Lieb theorem.¹⁶ However, for more general situations, one should rely on robust, accurate, and cost-effective theoretical methods, which is still a difficult task not exempted from computational limitations, especially for large systems.¹⁷

On the other hand, the application of standard Density Functional Theory (DFT) methods to these (poly)radical systems is known to be affected by some pitfalls and/or artifacts: the intrinsic one-determinantal nature of Kohn-Sham (KS) DFT precludes to deal with orbital degeneracies, thus neglecting non-dynamical or static correlation effects, and the use of a Broken-

1
2
3
4
5
6
7
8 Symmetry (BS) solution for open-shell systems introduces spin-contamination
9 (also scaling with size¹⁸) issues mostly affecting the energy of the low-spin
10 solution.¹⁹ This situation has historically prompted the development of non-
11 standard methods able to cope with these subtle electronic effects, namely
12 based on the two-body on-top pair density²⁰⁻²⁹ with a revisited interest
13 nowadays,³⁰⁻³³ the balanced coupling of *ab initio* and density functional
14 expressions,³⁴⁻³⁷ the use of natural orbitals³⁸⁻⁴⁰ or the specific *ensemble*
15 of pure spin states,⁴¹⁻⁴³ to name just a few of the existing non-standard
16 methods. Another possible route is the use of fractional spin⁴⁴ or orbital
17 occupation,^{45,46} mimicking the situation when multiconfigurational *ab ini-*
18 *tio* methods are instead employed, or spin-flip techniques,⁴⁷⁻⁴⁹ describing
19 target states from a high-spin reference state.
20
21
22
23
24
25
26
27
28
29
30

31 To further explore (*vide infra*) the applicability and accuracy of modern
32 DFT variants, in the search for the best trade-off between accuracy and
33 computational cost, we have chosen a set of large (and real-world) organic
34 radical compounds recently synthesized and crystallized with diverse struc-
35 tural motifs (see Figure 1). Note that for all of the systems selected, their
36 stability has allowed the original authors to perform experimental measure-
37 ments such as Electron Spin Resonance (ESR) or Superconducting QUan-
38 tum Interference Device (SQUID), among others, to extract e.g., the energy
39 difference between low- and high-spin states, thus allowing to bracket the
40 accuracy of the theoretical methods employed after the comparison with ex-
41 perimental results. The systems selected here (and their short names used
42 in the following) are: (i) substituted Blatter-like radicals^{50,51} (Diradical
43 I and II); (ii) [6]cyclo-para-phenylmethine⁵² (6CPPM-Mes); (iii) [n]cyclo-
44 para-biphenylmethines⁵³ ([n]CPBM-Ant) with $n = 3 - 6$; (iv) ethynylene-
45
46
47
48
49
50
51
52
53
54
55
56
57
58
59
60

1
2
3
4
5
6
7
8 bridged fluorenyl macrocycle⁵⁴ (MC-F3A3); and (v) cyclopenta-ring-fused
9 oligo(m-phenylene) macrocyclic⁵⁵ (8MC). Note that the DFT-based results
10 will also be compared with those from the Restricted-Active-Space Spin-
11 Flip (RAS-SF) method,⁵⁶ to bracket their accuracy also for magnitudes for
12 which experimental results are not available.
13
14
15
16
17
18

19 Theoretical Methods

20 The FT-DFT method

21
22
23
24 The Finite-Temperature DFT (FT-DFT) method relies on the fractional
25 occupation of molecular orbitals induced by (near-)degeneracy effects, with
26 the associated density written as:
27
28

$$29 \rho(\mathbf{r}) = \sum_i^{\infty} f_i |\phi_i(\mathbf{r})|^2, \quad (1)$$

30
31
32 where $\phi_i(\mathbf{r})$ is a molecular spin-orbital and f_i its fractional electron occupa-
33 tion numbers ($0 \leq f_i \leq 1$). The self-consistency of the procedure is achieved
34 by minimizing the Gibbs electronic free energy ($G_{el} = E_{el} - T_{el}S_{el}$) of the
35 system at a fictitious pseudo-temperature (i.e., electronic) called T_{el} , with
36 the f_i values obtained by a Fermi-Dirac distribution around the Fermi level
37 E_F :
38
39
40
41
42

$$43 f_i = \frac{1}{1 + e^{(\epsilon_i - E_F)/\theta}}, \quad (2)$$

44
45 depending on $\theta = k_B T_{el}$. The corresponding energy difference between the
46 low-spin (LS) and high-spin (HS) solutions can be calculated after impos-
47 ing the desired spin multiplicity, $\Delta E(\text{LS} - \text{HS}) = E(\text{LS}) - E(\text{HS})$, with
48 $\Delta E(\text{LS} - \text{HS}) < 0$ indicating a favoured low-spin ground-state (antiferro-
49 magnetic). Note the similarities between this method and the Thermally-
50 Assisted-Occupation (TAO) DFT method of Chai *et al.*^{46,57}
51
52
53
54
55
56
57
58
59
60

Characterization of the radical character

Additionally, the set $\{f_i, \phi_i(\mathbf{r})\}$ can be used to define a density of unpaired electrons, that is the Fractional Orbital Density (FOD)^{58,59} as:

$$\rho^{FOD}(\mathbf{r}) = \sum_i^M (\delta_1 - \delta_2 f_i) |\phi_i(\mathbf{r})|^2, \quad (3)$$

where δ_1 and δ_2 are chosen to become (1, 1) if the single-particle energy level (ϵ_i) associated with the orbital ϕ_i is lower than the energy of the Fermi level, E_F , or (0, -1) otherwise. This density also leads upon integration to a measure of the number of strongly correlated electrons, $N_{FOD} = \int \rho^{FOD}(\mathbf{r}) d\mathbf{r}$, which is a concept equivalent to the (linear) metrics introduced by Head-Gordon,⁶⁰ typically labelled as N_U and obtained from natural orbital occupation numbers (NOONs), i.e., the eigenvalues of the one-electron reduced density matrix.

Complementarily, the radical character of electronic states can be quantified by means of the radical indices $0 \leq y_i \leq 1$ ($i = 0, 1, 2, 3$). Within the FT-DFT methodology, they can be directly assigned to the electronic occupations above the Fermi level as $y_i = f_{LUMO+i}^\alpha + f_{LUMO+i}^\beta$, with f_{LUMO+i}^σ the fractional occupation number of the lowest unoccupied LUMO+ i spin-orbital (since approximately $f_{LUMO+i}^\sigma + f_{HOMO-i}^\sigma = 1$). For systems with a significant (poly)radical nature, the indices y_i can be used to estimate their di- or tri- (y_0), tetra- or penta- (y_1), hexa- or hepta- (y_2), and octa- or nonradical (y_3) character, respectively. Large indices ($y_i \approx 1$) indicate high radical character, while intermediate values are indicative of moderate (poly)radicaloid character. The similarity of these fractional occupation numbers with the NOONs has been recently confirmed for polycyclic aromatic hydrocarbons,⁶¹ as well as the trend between N_{FOD} and global

1
2
3
4
5
6
7
8 biradical values arising from experimental measurements.^{62,63}
9
10

11 The SF-DFT method

12
13
14 The Spin-Flip DFT (SF-DFT) method relies on the exchange of the
15 α and β spin blocks of the density on certain user-defined centers, thus
16 generating a Broken-Symmetry (BS) solution after converging the high-spin
17 wavefunction. The energy difference between both considered configurations
18 is given by $\Delta E(\text{BS} - \text{HS}) = E(\text{BS}) - E(\text{HS})$, which can be used as a first
19 approximation to the energy difference between LS and HS solutions. Energy
20 differences between pure spin states can be estimated by the Yamaguchi's
21 procedure:⁶⁴⁻⁶⁶
22
23
24
25
26
27
28

$$29 \Delta E(\text{LS} - \text{HS}) = \frac{n_S}{\langle \hat{S}^2 \rangle_{\text{HS}} - \langle \hat{S}^2 \rangle_{\text{BS}}} \Delta E(\text{BS} - \text{HS}), \quad (4)$$

30
31
32 where n_S corresponds to the $\langle \hat{S}^2 \rangle$ difference between the ideal spin multi-
33 plicities, e.g., $n_S = 2$ for a LS singlet and a HS triplet, $n_S = 3$ for a LS
34 doublet and a HS quartet, etc.
35
36
37
38

39 The SF-TDDFT method

40
41
42 The Spin-Flip Time-Dependent DFT (SF-TDDFT) method is recognized
43 to uniformly describe excited states of single, double, and mixed excita-
44 tion character in molecular systems,⁶⁷ and more specifically in conjugated
45 molecules featuring diradical or (poly)radical character,^{68,69} starting from
46 a high-spin (e.g., triplet) reference state. The formalism is based on the
47 (linear response) TDDFT equations for excitation energies:
48
49
50
51
52
53

$$54 \begin{bmatrix} \mathbf{A} & \mathbf{B} \\ \mathbf{B}^* & \mathbf{A}^* \end{bmatrix} \begin{bmatrix} \mathbf{X} \\ \mathbf{Y} \end{bmatrix} = \Omega \begin{bmatrix} \mathbf{1} & \mathbf{0} \\ \mathbf{0} & -\mathbf{1} \end{bmatrix} \begin{bmatrix} \mathbf{X} \\ \mathbf{Y} \end{bmatrix}, \quad (5)$$

with \mathbf{X} (\mathbf{Y}) the set of (de-)excitation amplitudes, \mathbf{A} and \mathbf{B} the linear-response matrices, and Ω the excitation energies. In SF-TDDFT, Eq. (5) is solved for the subspace of spin-flip ($\alpha \rightarrow \beta$) operators.⁴⁷ For this case, the general expression for \mathbf{A} and \mathbf{B} elements simplify to $A_{i\bar{a},j\bar{b}} = \delta_{ij}\delta_{\bar{a},\bar{b}}(\epsilon_{\bar{a}} - \epsilon_i) - C_x(ij|\bar{a}\bar{b})$ and $B_{i\bar{a},j\bar{b}} = -C_x(ib|\bar{a}\bar{j})$, with C_x the weight of exact exchange of the density functional used, i, j (a, b) refer to occupied (virtual) orbitals (the overbar on orbital indices indicates β -spin), ϵ_p is the energy associated to the KS p -spin-orbital, and $(pq|st)$ is the two electron interaction integral given in Mülliken's notation:

$$(pq|st) = \int \phi_p^*(\mathbf{x})\phi_q(\mathbf{x})\frac{1}{|\mathbf{x} - \mathbf{x}'|}\phi_t^*(\mathbf{x}')\phi_s(\mathbf{x}')d\mathbf{x}d\mathbf{x}' \quad (6)$$

The RAS-SF method

Spin-flip methods with single spin-flip excitations⁷⁰⁻⁷² are not capable to properly describe low-spin states of molecular systems with more than three unpaired electrons, e.g., tetradicals. This limitation can be overcome through the generalization of the excitation operator to multiple spin-flip excitations, as in the RAS-SF method. In RAS-SF the orbital space of the high-spin reference is split in three subspaces: doubly occupied (RAS1), singly occupied (RAS2), and virtual (RAS3). The eigenstates of the RAS-SF Hamiltonian are obtained as n -spin-flip excitations expanded in terms of the number of holes (electrons) in the doubly (virtual) spaces:

$$\hat{R}^{n\text{SF}} = \hat{r}_0^{n\text{SF}} + \hat{r}_h^{n\text{SF}} + \hat{r}_p^{n\text{SF}} + \hat{r}_{hp}^{n\text{SF}} + \hat{r}_{2h}^{n\text{SF}} + \hat{r}_{2p}^{n\text{SF}} + \dots, \quad (7)$$

where $\hat{r}_0^{n\text{SF}}$ performs all possible spin-flip excitations within RAS2 and h and p subindices indicate the number of holes and electrons in RAS1 and

RAS3, respectively.

Computational details

We use a semi-local (TPSS⁷³) and a pair of hybrid⁷⁴ (TPSS0 and TPSSHH) exchange-correlation meta-GGA functionals differing in the weight (C_x) of the EXact-eXchange (EXX) introduced (i.e., 0% for TPSS, 25% for TPSS0, and 50% for TPSSHH) for the FT-DFT and SF-DFT calculations reported here. Note that the original FT-DFT method employed the TPSS functional, which will be respected here, but we will also complementarily explored the dependence of the results with respect to the EXX weight. The electronic temperature (T_{el}) was fixed for the FT-DFT calculations following the recommended expression $T_{el}/K = 5000 + 20000 C_x$ as a function of the EXX weight C_x .

We use the cost-effective 6-31G** (SF-DFT) and the large def2-TZVP⁷⁵ (FT-TPSS) basis sets for those calculations, together with the RIJCOSX technique⁷⁶ (with the def2/JK auxiliary basis sets⁷⁷) to reduce the increase in computational cost associated to the TPSS0 and TPSSHH functionals. The plots of the $\rho^{\text{FOD}}(\mathbf{r})$ density were generated by the UCSF Chimera⁷⁸ (version 1.12) package. The FT-DFT and SF-DFT calculations were done with the ORCA (version 4.0.1.2) quantum-chemical package⁷⁹ employing ultrafine numerical integration grids (i.e., Grid6, NoFinalGrid) in all cases.

The SF-TDDFT calculations employed the collinear approximation as implemented in the GAMESS package,⁸⁰ together with the BHHLYP functional⁸¹ and the cost-effective 6-31G* basis set. Note that the use of a functional with a high $C_x = 0.50$ value is recommended for this kind of

1
2
3
4
5
6
7
8 calculations,^{47,82} and that the accuracy is not expected to vary using an-
9 other exchange-correlation functional like TPSSHH or PBEHH (both with
10 the same $C_x = 0.50$ value than BHHLYP).⁸³
11
12
13
14

15 The RAS-SF calculations have been done within the hole and electron
16 approximation, that is including the three first terms in the rhs of Eq. (5)
17 using a ROHF (Restricted Open-Shell) high-spin reference: triplet (Blatter-
18 like diradicals), quartet ([3]CPBM), quintet ([4]CPBM), sextet ([5]CPBM),
19 septet ([6]CPPM and [6]CPBM), and nonet (8MC). Further details can be
20 found at the Supporting Information and elsewhere.⁵²⁻⁵⁵ These calculations
21 have been done with the Q-Chem (version 5.2) program⁸⁴ and the 6-31G**
22 basis set.
23
24
25
26
27
28
29
30

31 Finally, the Zero-Field-Splitting (ZFS) calculations were performed with
32 the ω B97X-D functional⁸⁵ and the IGLO-II basis set,⁸⁶ intended for com-
33 puting magnetic properties with high accuracy,⁸⁷ together with the 'Au-
34 toAux' generation procedure for auxiliary basis sets.⁸⁸ The ZFS tensor was
35 self-consistently calculated on the basis on spin-Unrestricted Natural Or-
36 bitals (UNO)⁸⁹ as recommended.⁹⁰ The ZFS calculations were done with
37 the ORCA (version 4.0.1.2) quantum-chemical package⁷⁹ employing a tight
38 threshold for convergence (i.e., TightSCF) and ultrafine numerical integra-
39 tion grids (i.e., Grid6, NoFinalGrid) in all cases.
40
41
42
43
44
45
46
47
48
49
50
51
52
53
54
55
56
57
58
59
60

Results and discussion

Quantification of the (poly)radicaloid character.

First, we aim to evaluate the extent of the radical character, i.e., the number of unpaired electrons (N_{FOD}), of the considered molecular species by means of FT-DFT calculations. The N_{FOD} values obtained by FT-TPSS, FT-TPSS0, and FT-TPSSHH methods are presented in Table 1 for both the low- and high-spin states of all studied compounds. Complementarily, Figure 2 compares the calculated N_{FOD} values for the low-spin state of all compounds, from which we can recognize a close agreement between RAS-SF and FT-TPSS results. The results discussed along this section will thus limit to those obtained at the FT-TPSS level, with FT-TPSS0 slightly (FT-TPSSHH largely) overestimating the RAS-SF results. Moreover, all molecules present significant N_{FOD} values, indicating their open-shell (poly)radical character. The radical character is also preserved for the high-spin states, i.e. qualitatively similar $N_{FOD}(\text{LS})$ and $N_{FOD}(\text{HS})$ values are found except for Diradical I and II systems. Because fractional occupation is induced by near degeneracy, the smaller values of N_{FOD} for the HS state of Diradical I and II can be rationalized by their HOMO-1/HOMO and LUMO/LUMO+1 gaps, considerably larger than those of the other systems investigated. Interestingly, the series of [n]CPBM-Ant ($n = 3 - 6$) compounds is predicted to increase their radical character as a function of their increasing size, in perfect agreement with experimental and RAS-SF results.⁵³

Following the agreement found between N_{FOD} values at the FT-TPSS and RAS-SF levels, see also Table S1, we represent in Figure 3 the topology (real-space distribution) of the corresponding density, $\rho^{FOD}(\mathbf{r})$, at the FT-TPSS level and using the recommended threshold^{58,59} for the isocon-

1
2
3
4
5
6
7
8 tour values ($\sigma = 0.005 \text{ e/bohr}^3$). For the Blatter-like radicals, the FOD
9 density concentrates on the N atoms of the conjugated backbone, and on
10 the nitrosyl substituents, in agreement with what one would expect from the
11 resonance Lewis structures of the molecules. For 6CPPM-Mes, [n]CPBM-
12 Ant ($n = 3 - 6$), and MC-F3A3 compounds we can observe how the FOD
13 density locates mainly at those C atoms bringing the mesityl and anthracene
14 substituents, respectively, acting effectively as protective synthons. For the
15 8MC compound we observe a delocalization of the FOD density on the non-
16 bridging C atoms, resembling the results found for other systems with cyclic
17 topologies as cyclacenes (i.e. cyclic oligoacenes⁹¹).
18
19
20
21
22
23
24
25
26
27

28 **Radical(oid) indices.**

29
30 In order to get a deeper insight into the radical nature of these com-
31 pounds, in the following we explore them by means of their $\{y_i\}$ indices.
32 Table 2 presents the y_0 , y_1 , y_2 , and y_3 values for all the systems studied at
33 the FT-TPSS level. The Blatter-like diradicals exhibit nearly ideal diradical
34 character, with $y_0 \simeq 1.0$ and $y_{i>0} \simeq 0$ for the low and high-spin T_0 states.
35 Note that this is in agreement with the smaller N_{FOD} values discussed in
36 the previous section for the HS state of these two systems. The 6CPPM-Mes
37 molecule holds a sizable tetraradicaloid character, with moderate y_0 and y_1
38 values for the ground-state singlet. For the [n]CPBM-Ant ($n = 3 - 6$) sys-
39 tems, we observe an increase of the number of strongly correlated electrons
40 as a function of their size, in agreement with the trend found for the N_{FOD}
41 values. Inspection of their y_i values allows to classify them as tri-, tetra-
42 , penta- and hexaradicaloid molecules, respectively. Finally, for the 8MC
43 molecule we obtain moderate values for all the y_{0-3} indices, indicating a
44 moderate octaradicaloid behaviour. Tables S2-S3 present the y_i values ob-
45
46
47
48
49
50
51
52
53
54
55
56
57
58
59
60

1
2
3
4
5
6
7
8 tained at the FT-TPSS0 and FT-TPSSHH levels, respectively, which follow
9 the same trend found for FT-TPSS, but with $\{y_i\}$ indices being systemati-
10 cally larger, like for N_{FOD} values.
11
12

13 14 15 **Energy difference between low- and high-spin states.** 16

17
18 Table 3 presents the energy difference $\Delta E(\text{LS} - \text{HS})$ between the low-
19 and high-spin states of all the systems considered, calculated at the FT-
20 TPSS, FT-TPSS0, and FT-TPSSHH levels. Note that, except for the Blatter-
21 like diradicals considered, the electronic ground-state of these systems is al-
22 ways the one with the lowest spin-multiplicity, thus denoted as S_0 (singlet) or
23 D_0 (doublet). Therefore, $\Delta E(\text{LS} - \text{HS})$ refers to the S_0 - T_1 or D_0 - Q_1 energy
24 difference, respectively, and will hold a negative sign: $\Delta E(\text{LS} - \text{HS}) < 0$.
25 For the Blatter-like diradicals, the triplet electronic ground-state is instead
26 favoured, and in these cases it should be $\Delta E(\text{LS} - \text{HS}) > 0$ accordingly.
27 First of all, inspecting the evolution of values in Table 3, we can see how
28 the relative stabilization of the HS state with respect to the LS solution
29 increases with the amount of Hartree-Fock exchange, i.e., upon going from
30 FT-TPSS to FT-TPSS0, and to FT-TPSSHH, with the latter being system-
31 atically closer to experimental energy gaps. This behaviour agrees with the
32 benchmark studies dealing with transition metal complexes.⁹²⁻⁹⁴ However,
33 the agreement with experimental results largely differs among the set of
34 compounds, even looking at the FT-TPSSHH results (i.e. best estimates)
35 providing the lowest MSE and MUE values. For [6]CPBM or 8MC, employ-
36 ing any of the FT-DFT variants will lead to an error close or even less than
37 1 kcal/mol, commonly known as the chemical accuracy threshold. On the
38 other hand, for [3]CPBM and MC-F3A3 compounds the computed gaps are
39 a few kcal/mol too negative, even with the FT-TPSSH method. Figure 4
40
41
42
43
44
45
46
47
48
49
50
51
52
53
54
55
56
57
58
59
60

1
2
3
4
5
6
7
8 compares the FT-DFT calculated values with the experimental results, for
9 which we can also easily observe a different behaviour for odd and even
10 $[n]$ CPBM compounds. These facts, together with the spread of the results
11 for MC-F3A3, allow us to conclude that the FT-DFT (with the default elec-
12 tronic temperatures) tends to overestimate the relative stability of low-spin
13 (singlet or doublet) state with respect to the next higher spin state (triplet
14 or quartet). Energy differences can be systematically improved, to some
15 extend, by increasing the amount of exact exchange.
16
17
18
19
20
21
22
23

24 We compare next the SF-DFT and the experimental results in Table
25 4, also using the TPSS, TPSS0, and TPSSHH functionals to disclose the
26 effect of linearly increasing the exact-exchange weight. First of all, we con-
27 sider the FOD density as the criteria to select those atoms to flip, with the
28 highest density localized on them, which could also be roughly estimated by
29 inspecting the corresponding spin density. In this case, spin contamination
30 becomes a key factor and results progressively deteriorates upon increas-
31 ing the exact-exchange weight, contrarily to what happened with FT-DFT
32 methods. The (spin-corrected) energy gaps $\Delta E(\text{LS} - \text{HS})$ keep an accuracy
33 similar to that obtained for the uncorrected $\Delta E(\text{BS} - \text{HS})$ values, still with
34 the SF-TPSS or SF-TPSS0 methods providing the closest agreement with
35 experimental results (e.g., MUEs of 6.0 and 4.0–5.0 kcal/mol, respectively).
36 Remarkably, the SF-TPSS method provides the correct lowest-energy spin-
37 state for all the molecules considered, contrarily to SF-TPSS0 and especially
38 SF-TPSSHH. Inspecting now the SF-TDDFT results in Table 5, done with
39 the BHHLYP and thus comparable with TPSSHH in terms of having a sim-
40 ilar exact exchange proportion, we observe larger averaged errors than for
41 previous FT-DFT or SF-DFT methods, with a reverse state ordering for
42
43
44
45
46
47
48
49
50
51
52
53
54
55
56
57
58
59
60

Diradicals I and II. The method yields too large energy differences for the set of $[n]$ CPBM compounds, but it keeps the correct trend of decreasing the ΔE values with increasing size.

For the sake of comparison of all these results, RAS-SF gives a MSE (MUE) of -0.55 (0.85) kcal/mol with respect to experimental results, with a maximum deviation of 3.2 kcal/mol and producing thus more accurate relative energies than the investigated DFT-based methods. Actually, this method is able to provide the chemical accuracy sought for the whole set of compounds. Discarding the case of $[6]$ CPPM-Mes, the MSE (MUE) would decrease to -0.22 (0.56) kcal/mol, and thus being considerably low.

Zero-field splitting interactions

The magnetic dipole-dipole (i.e., spin-spin) interaction leads to the splitting of the triplet sublevels ($M_s = 0, \pm 1$) even in the absence of any external field; a physical effect described by the Zero-Field Splitting (ZFS) Hamiltonian:

$$\hat{H}_{ZFS} = \hat{\mathbf{S}} \cdot \hat{\mathbf{D}} \cdot \hat{\mathbf{S}} = D_{xx} \hat{S}_x^2 + D_{yy} \hat{S}_y^2 + D_{zz} \hat{S}_z^2 = D \left(\hat{S}_z^2 - \frac{1}{3} \hat{\mathbf{S}}^2 \right) + E \left(\hat{S}_x^2 - \hat{S}_y^2 \right), \quad (8)$$

with D_{ii} the principal values of the ZFS diagonal tensor $\hat{\mathbf{D}}$, which by convention are recasted as:

$$D = D_{zz} - \frac{1}{2} (D_{xx} + D_{yy}), \quad (9)$$

$$E = \frac{1}{2} (D_{xx} - D_{yy}). \quad (10)$$

For systems having $S > 1/2$, the ZFS usually dominates the spectral shape of the Electron Paramagnetic Resonance (EPR) spectra, and thus the absolute values of D and the E/D ratio determine the energies of the three

1
2
3
4
5
6
7
8 magnetic sublevels.⁹⁵ Additionally, provided that the point-dipole approxi-
9 mation holds, D also relates with the averaged distance (Δr) between ide-
10 ally localized spin densities, and can be thus used to estimate the size of the
11 photoexcited triplet exciton⁹⁶ (see the Supporting Information for further
12 details). Note that in the following we will restrict the study to those sys-
13 tems possessing ground-state or low-lying triplet states, i.e., with an even
14 number of electrons.
15
16
17
18
19
20
21

22 First of all, we have thoroughly assessed the accuracy of DFT methods
23 to calculate the D and E parameters for the pair of systems (Diradicals
24 I and II) for which experimental measurements are available.⁵¹ For both
25 compounds it is clear that $D/hc < 0$ from the experimental EPR spec-
26 tra, thus indicating a prolate-like distribution of the spin density for the
27 triplet state. The sign of D indicates whether the $M_s = 0$ ($D > 0$) or
28 $M_s = \pm 1$ ($D < 0$) spin substrates are the lowest energy states at zero ex-
29 ternal fields. However, previous results at the B3LYP/EPR-II level,⁵¹ and
30 with different exchange-correlation functionals and basis sets (see Tables S4-
31 S5), predicted the wrong sign for Diradical II ($D/hc > 0$), which is properly
32 characterized only by certain range-separated functionals (i.e., ω B97X-D⁸⁵
33 and LC-BLYP⁹⁷) together with basis sets suited for electric and magnetic
34 properties, i.e. IGLO-II or EPR-II, previously applied⁹⁸ to the study of
35 spin-spin contributions to the ZFS tensor in organic radicals too.
36
37
38
39
40
41
42
43
44
45
46
47
48

49 This deficiency of DFT methods has also been documented before^{99,100}
50 and prompted us to apply in the following the ω B97X-D functional for con-
51 sistency. Note also that the range-separated CAM-B3LYP functional¹⁰¹ was
52 also used but did not bring the correct sign of D for Diradical II. The main
53
54
55
56
57
58
59
60

1
2
3
4
5
6
7
8 difference between the ω B97X-D/LC-BLYP and CAM-B3LYP schemes is a
9 relatively large (35%) fixed DFT exchange contribution in the latter, and
10 thus a maximum screened exact exchange of 65%, which seems to corrob-
11 orate the importance of that variable part (80% and 100% for ω B97X-D
12 and LC-BLYP, respectively). On the other hand, looking again at Tables
13 S4-S5, the relative error for the calculation of E was found larger than for
14 D , in agreement with previous applications to heavy-atoms coordination
15 complexes.¹⁰²
16
17
18
19
20
21
22
23

24 Table 6 presents the D , E , and Δr calculated values (at the ω B97X-
25 D/IGLO-II level) for the lowest triplet state of the set of compounds studied.
26 Interestingly, for the Diradicals I and II, a high-spin ground-state together
27 with a negative D could lead to effective molecular magnets.¹³ In the case
28 of 8MC, we can see how $E = 0$ due to the perfect axial symmetry of this
29 compound, with E being considerably lower than D as expected in all other
30 cases. Inspecting the Δr values, i.e., the mean inter-spin distance in a dipole-
31 dipole approximation, see the Supporting Information for further details
32 about the explicit derivation, we can see how it decreases with the system
33 size; a fact also documented before for linear polyenes and polyacenes.¹⁰³
34 This is rationalized by the dependence $D \propto r^{-3}$ with r the distance between
35 the spins of the unpaired electrons. We can also compare these results with
36 the estimated exciton size (Δr) for the triplet ground-state of 2,6,10-Tri-
37 *tert*-Butyltriangulene,¹⁰⁴ around 5.6 Å, or for the photoexcited triplet state
38 of tetracene and pentacene,¹⁰⁵ around 3.8 Å, or for the photoexcited triplet
39 state of B- and N-doped nanographenes,¹⁰⁶ around 4.4-5.2 Å depending on
40 their size.
41
42
43
44
45
46
47
48
49
50
51
52
53
54
55
56
57
58
59
60

Conclusions

We report here a benchmark study of a set of real-world (poly)radicaloids, focusing on the extent of the radical character, spatial distribution of the unpaired electrons, and singlet-triplet (or doublet-quartet) energy difference obtained with different electronic structure methods. Current research on organic (poly)radicaloid character and its applications has prompted the application here of both (cost-effective) DFT-based and RAS-SF methods, with the latter method behaving more accurately than the others as compared with reference experimental results. Complementarily, we have systematically compared finite-temperature (FT-DFT) and spin-flip approaches (SF-DFT and SF-TDDFT) with various exchange-correlation functionals, mostly differing in their exact exchange weight, to disentangle the effect of the underlying expression as well as the effect of the spin-contamination introduced. The use of any of these approaches with a meta-GGA form (i.e., TPSS) is less costly than using a hybrid expression, but errors calculated at the FT-TPSSHH or SF-TPSS0 level are lower than those calculated with the corresponding non-hybrid versions (i.e., FT-TPSS or SF-TPSS). Finally, we have also calculated the ZFS parameters for the triplet states of the compounds, as well as their exciton size. Overall, we have shown how the cost-effective characterization of (poly)radicaloid nature in conjugated organic compounds is still a challenging issue, precluding the blind application of DFT variants.

Acknowledgements

G.S. acknowledges the Erasmus+ program for a research internship. D.C. is thankful to projects PIBA19-0004 (Eusko Jaurlaritza) and CTQ2016-

80955-P from the Spanish Government (MINECO/FEDER).

Supplementary Material

The Supplementary Material contains in this order: (i) the metrics error used to compare the performance of the different methods; (ii) N_U and $\Delta E(\text{LS} - \text{HS})$ values obtained at the RAS-SF level for all the compounds; (iii) calculated radical indices (y_i) at the FT-TPSS0 and FT-TPSSH levels for all the compounds; (iv) comparison between calculated and experimental EPR parameters for Diradicals I and II; (v) notes on the theoretical estimates of the exciton size and the sign of the D-tensor; (vi) cartesian coordinates of all the compounds.

References

- [1] Hu, X.; Wang, W.; Wang, D.; Zheng, Y. The electronic applications of stable diradicaloids: present and future. *Journal of Materials Chemistry C* **2018**, *6*, 11232–11242.
- [2] Badía-Domínguez, I.; Pérez-Guardiola, A.; Sancho-García, J. C.; Lopez Navarrete, J. T.; Hernandez Jolin, V.; Li, H.; Sakamaki, D.; Seki, S.; Rúa Delgado, M. C. Formation of Cyclophane Macrocycles in Carbazole-Based Biradicaloids: Impact of the Dicyanomethylene Substitution Position. *ACS Omega* **2019**, *4*, 4761–4769.
- [3] Morita, Y.; Suzuki, S.; Sato, K.; Takui, T. Synthetic organic spin chemistry for structurally well-defined open-shell graphene fragments. *Nature chemistry* **2011**, *3*, 197.
- [4] Pavliček, N.; Mistry, A.; Majzik, Z.; Moll, N.; Meyer, G.; Fox, D. J.;

- 1
2
3
4
5
6
7
8 Gross, L. Synthesis and characterization of triangulene. *Nature Nanotechnology* **2017**, *12*, 308.
- 9
10
11
12 [5] Wang, S.; Talirz, L.; Pignedoli, C. A.; Feng, X.; Müllen, K.; Fasel, R.;
13 Ruffieux, P. Giant edge state splitting at atomically precise graphene
14 zigzag edges. *Nature Communications* **2016**, *7*, 11507.
- 15
16
17
18 [6] Li, J.; Sanz, S.; Corso, M.; Choi, D. J.; Peña, D.; Frederiksen, T.;
19 Pascual, J. I. Single spin localization and manipulation in graphene
20 open-shell nanostructures. *Nature Communications* **2019**, *10*, 200.
- 21
22
23
24 [7] Pozo, I.; Majzik, Z.; Pavliček, N.; Melle-Franco, M.; Guitián, E.;
25 Peña, D.; Gross, L.; Perez, D. Revisiting kekulene: synthesis and
26 single-molecule imaging. *Journal of the American Chemical Society*
27 **2019**, *141*, 15488–15493.
- 28
29
30
31
32 [8] Mondal, R.; Shah, B. K.; Neckers, D. C. Photogeneration of heptacene
33 in a polymer matrix. *Journal of the American Chemical Society* **2006**,
34 *128*, 9612–9613.
- 35
36
37
38 [9] Tönshoff, C.; Bettinger, H. F. Photogeneration of octacene and
39 nonacene. *Angewandte Chemie International Edition* **2010**, *49*, 4125–
40 4128.
- 41
42
43
44 [10] Segawa, Y.; Yagi, A.; Matsui, K.; Itami, K. Design and Synthesis of
45 carbon nanotube segments. *Angewandte Chemie International Edition*
46 **2016**, *55*, 5136–5158.
- 47
48
49
50
51 [11] Povie, G.; Segawa, Y.; Nishihara, T.; Miyauchi, Y.; Itami, K. Synthesis
52 of a carbon nanobelt. *Science* **2017**, *356*, 172–175.
- 53
54
55
56 [12] Stuyver, T.; Chen, B.; Zeng, T.; Geerlings, P.; De Proft, F.; Hoff-

- mann, R. Do Diradicals Behave Like Radicals? *Chemical Reviews* **2019**,
- [13] Perumal, S.; Minaev, B.; Ågren, H. Spin-spin and spin-orbit interactions in nanographene fragments: A quantum chemistry approach. *The Journal of Chemical Physics* **2012**, *136*, 104702.
- [14] Ortiz, R.; Boto, R. Á.; García-Martínez, N.; Sancho-García, J. C.; Melle-Franco, M.; Fernández-Rossier, J. Exchange rules for diradical π -conjugated hydrocarbons. *Nano Letters* **2019**, *19*, 5991–5997.
- [15] Ovchinnikov, A. A. Multiplicity of the ground state of large alternant organic molecules with conjugated bonds. *Theoretica Chimica Acta* **1978**, *47*, 297–304.
- [16] Lieb, E. H. Two theorems on the Hubbard model. *Physical Review Letters* **1989**, *62*, 1201.
- [17] Das, A.; Muller, T.; Plasser, F.; Lischka, H. Polyradical Character of Triangular Non-Kekulé Structures, Zethrenes, p-Quinodimethane-Linked Bisphenalenyl, and the Clar Goblet in Comparison: An Extended Multireference Study. *The Journal of Physical Chemistry A* **2016**, *120*, 1625–1636.
- [18] Hajgató, B.; Deleuze, M. S. Quenching of magnetism in hexagonal graphene nanoflakes by non-local electron correlation. *Chemical Physics Letters* **2012**, *553*, 6–10.
- [19] Illas, F.; Moreira, I. P.; De Graaf, C.; Barone, V. Magnetic coupling in biradicals, binuclear complexes and wide-gap insulators: a survey of ab initio wave function and density functional theory approaches. *Theoretical Chemistry Accounts* **2000**, *104*, 265–272.

- 1
2
3
4
5
6
7
8 [20] Moscardó, F.; San-Fabián, E. Density-Functional Formalism and the
9 Two-Body Problem. *Physical Review A* **1991**, *44*, 1549.
10
11
12 [21] Perdew, J. P.; Savin, A.; Burke, K. Escaping the Symmetry Dilemma
13 through a Pair-Density Interpretation of Spin-Density Functional The-
14 ory. *Physical Review A* **1995**, *51*, 4531.
15
16
17 [22] Miehlich, B. B.; Stoll, H.; Savin, A. A Correlation-Energy Density
18 Functional for Multideterminantal Wavefunctions. *Molecular Physics*
19 **1997**, *91*, 527–536.
20
21
22 [23] Moscardó, F.; Pérez-Jiménez, A. J. Self-Consistent Field Calculations
23 Using Two-Body Density Functionals for Correlation Energy Compo-
24 nent: I. Atomic Systems. *Journal of Computational Chemistry* **1998**,
25 *19*, 1887–1898.
26
27
28 [24] Moscardó, F.; Pérez-Jiménez, A. J.; Cjuno, J. A. Self-Consistent Field
29 Calculations Using Two-Body Density Functionals for Correlation
30 Energy Component: II. Small Molecules. *Journal of Computational*
31 *Chemistry* **1998**, *19*, 1899–1908.
32
33
34 [25] McDouall, J. J. Combining Two-Body Density Functionals with
35 Multiconfigurational Wavefunctions: Diatomic Molecules. *Molecular*
36 *Physics* **2003**, *101*, 361–371.
37
38
39 [26] Sancho-García, J. C.; Moscardó, F. Usefulness of the Colle–Salvetti
40 Model for the Treatment of the Nondynamic Correlation. *The Journal*
41 *of Chemical Physics* **2003**, *118*, 1054–1058.
42
43
44 [27] Takeda, R.; Yamanaka, S.; Yamaguchi, K. Approximate On-Top Pair
45 Density into One-Body Functions for CAS-DFT. *International Journal*
46 *of Quantum Chemistry* **2004**, *96*, 463–473.
47
48
49
50
51
52
53
54
55
56
57
58
59
60

- 1
2
3
4
5
6
7
8 [28] Gusarov, S.; Malmqvist, P.-Å.; Lindh, R. Using On-Top Pair Den-
9 sity for Construction of Correlation Functionals for Multideterminant
10 Wave Functions. *Molecular Physics* **2004**, *102*, 2207–2216.
11
12
13
14 [29] Toulouse, J.; Colonna, F.; Savin, A. Long-Range–Short-Range Sepa-
15 ration of the Electron-Electron Interaction in Density-Functional The-
16 ory. *Physical Review A* **2004**, *70*, 062505.
17
18
19
20 [30] Li Manni, G.; Carlson, R. K.; Luo, S.; Ma, D.; Olsen, J.; Truh-
21 lar, D. G.; Gagliardi, L. Multiconfiguration Pair-Density Functional
22 Theory. *Journal of Chemical Theory and Computation* **2014**, *10*,
23 3669–3680.
24
25
26
27
28 [31] Gagliardi, L.; Truhlar, D. G.; Li Manni, G.; Carlson, R. K.;
29 Hoyer, C. E.; Bao, J. L. Multiconfiguration Pair-Density Functional
30 Theory: A New Way to Treat Strongly Correlated Systems. *Accounts*
31 *of Chemical Research* **2016**, *50*, 66–73.
32
33
34
35
36 [32] Hoyer, C. E.; Ghosh, S.; Truhlar, D. G.; Gagliardi, L. Multiconfig-
37 uration Pair-Density Functional Theory is as Accurate as CASPT2
38 for Electronic Excitation. *The Journal of Physical Chemistry Letters*
39 **2016**, *7*, 586–591.
40
41
42
43
44 [33] Ghosh, S.; Cramer, C. J.; Truhlar, D. G.; Gagliardi, L. Generalized-
45 Active-Space Pair-Density Functional Theory: An Efficient Method
46 to Study Large, Strongly Correlated, Conjugated Systems. *Chemical*
47 *Science* **2017**, *8*, 2741–2750.
48
49
50
51
52 [34] Grimme, S.; Waletzke, M. A Combination of Kohn–Sham Density
53 Functional Theory and Multi-Reference Configuration Interaction
54 Methods. *The Journal of Chemical Physics* **1999**, *111*, 5645–5655.
55
56
57
58
59
60

- 1
2
3
4
5
6
7
8 [35] Gräfenstein, J.; Cremer, D. The Combination of Density Func-
9 tional Theory with Multi-Configuration Methods–CAS-DFT. *Chemical*
10 *Physics Letters* **2000**, *316*, 569–577.
11
12
13
14 [36] Nakata, K.; Ukai, T.; Yamanaka, S.; Takada, T.; Yamaguchi, K.
15 CASSCF Version of Density Functional Theory. *International Jour-*
16 *nal of Quantum Chemistry* **2006**, *106*, 3325–3333.
17
18
19
20 [37] Pijeau, S.; Hohenstein, E. G. Improved Complete Active Space Con-
21 figuration Interaction Energies with a Simple Correction from Den-
22 sity Functional Theory. *Journal of Chemical Theory and Computation*
23 **2017**, *13*, 1130–1146.
24
25
26
27
28 [38] Pérez-Jiménez, Á. J.; Pérez-Jordá, J. M.; Sancho-García, J. C. Com-
29 bining Two-Body Density Correlation Functionals with Multiconfigu-
30 rational Wave Functions Using Natural Orbitals and Occupation Num-
31 bers. *The Journal of Chemical Physics* **2007**, *127*, 104102.
32
33
34
35
36 [39] Piris, M.; Lopez, X.; Ruipérez, F.; Matxain, J.; Ugalde, J. A Natu-
37 ral Orbital Functional for Multiconfigurational States. *The Journal of*
38 *Chemical Physics* **2011**, *134*, 164102.
39
40
41
42 [40] Piris, M.; Ugalde, J. M. Perspective on Natural Orbital Functional
43 Theory. *International Journal of Quantum Chemistry* **2014**, *114*,
44 1169–1175.
45
46
47
48 [41] Filatov, M.; Shaik, S. A Spin-Restricted Ensemble-Referenced Kohn–
49 Sham Method and its Application to Diradicaloid Situations. *Chemical*
50 *Physics Letters* **1999**, *304*, 429–437.
51
52
53
54 [42] Kazaryan, A.; Heuver, J.; Filatov, M. Excitation Energies from
55 Spin-Restricted Ensemble-Referenced Kohn–Sham Method: A State-
56
57
58
59
60

- 1
2
3
4
5
6
7
8 Average Approach. *The Journal of Physical Chemistry A* **2008**, *112*,
9 12980–12988.
- 10
11
12 [43] Filatov, M. Spin-Restricted Ensemble-Referenced Kohn–Sham
13 Method: Basic Principles and Application to Strongly Correlated
14 Ground and Excited States of Molecules. *Wiley Interdisciplinary*
15 *Reviews: Computational Molecular Science* **2015**, *5*, 146–167.
- 16
17
18 [44] Ess, D. H.; Johnson, E. R.; Hu, X.; Yang, W. Singlet- Triplet Energy
19 Gaps for Diradicals from Fractional-Spin Density-Functional Theory.
20 *The Journal of Physical Chemistry A* **2010**, *115*, 76–83.
- 21
22
23 [45] Grimme, S. Towards First Principles Calculation of Electron Impact
24 Mass Spectra of Molecules. *Angewandte Chemie International Edition*
25 **2013**, *52*, 6306–6312.
- 26
27
28 [46] Chai, J.-D. Density Functional Theory with Fractional Orbital Occu-
29 pations. *The Journal of Chemical Physics* **2012**, *136*, 154104.
- 30
31
32 [47] Shao, Y.; Head-Gordon, M.; Krylov, A. I. The spin–flip approach
33 within time-dependent density functional theory: Theory and appli-
34 cations to diradicals. *The Journal of Chemical Physics* **2003**, *118*,
35 4807–4818.
- 36
37
38 [48] Wang, F.; Ziegler, T. Time-dependent density functional theory based
39 on a noncollinear formulation of the exchange-correlation potential.
40 *The Journal of Chemical Physics* **2004**, *121*, 12191–12196.
- 41
42
43 [49] Wang, F.; Ziegler, T. The performance of time-dependent density func-
44 tional theory based on a noncollinear exchange-correlation potential
45 in the calculations of excitation energies. *The Journal of Chemical*
46 *Physics* **2005**, *122*, 074109.
- 47
48
49
50
51
52
53
54
55
56
57
58
59
60

- 1
2
3
4
5
6
7
8 [50] Gallagher, N. M.; Bauer, J. J.; Pink, M.; Rajca, S.; Rajca, A. High-
9 spin organic diradical with robust stability. *Journal of the American*
10 *Chemical Society* **2016**, *138*, 9377–9380.
11
12
13
14 [51] Gallagher, N.; Zhang, H.; Junghoefer, T.; Giangrisostomi, E.; Ovsyan-
15 nikov, R.; Pink, M.; Rajca, S.; Casu, M. B.; Rajca, A. Thermally
16 and magnetically robust triplet ground state diradical. *Journal of the*
17 *American Chemical Society* **2019**, *141*, 4764–4774.
18
19
20
21
22 [52] Li, Z.; Gopalakrishna, T. Y.; Han, Y.; Gu, Y.; Yuan, L.; Zeng, W.;
23 Casanova, D.; Wu, J. [6]Cyclo-para-phenylmethine: an analog of ben-
24 zene showing global aromaticity and open-shell diradical character.
25 *Journal of the American Chemical Society* **2019**, *141*, 16266–16270.
26
27
28
29
30 [53] Ni, Y.; Sandoval-Salinas, M. E.; Tanaka, T.; Phan, H.; Heng, T. S.;
31 Gopalakrishna, T. Y.; Ding, J.; Osuka, A.; Casanova, D.; Wu, J.
32 [n]Cyclo-para-biphenylmethine polyradicaloids: [n]annulene analogs
33 and unusual valence tautomerization. *Chem* **2019**, *5*, 108–121.
34
35
36
37
38 [54] Lu, X.; Lee, S.; Hong, Y.; Phan, H.; Gopalakrishna, T. Y.;
39 Heng, T. S.; Tanaka, T.; Sandoval-Salinas, M. E.; Zeng, W.; Ding, J.;
40 Casanova, D.; Osuka, A.; Kim, D.; Wu, J. Fluorenyl based macrocyclic
41 polyradicaloids. *Journal of the American Chemical Society* **2017**, *139*,
42 13173–13183.
43
44
45
46
47
48 [55] Liu, C.; Sandoval-Salinas, M. E.; Hong, Y.; Gopalakrishna, T. Y.;
49 Phan, H.; Aratani, N.; Heng, T. S.; Ding, J.; Yamada, H.; Kim, D.;
50 Casanova, D.; Wu, J. Macrocyclic polyradicaloids with unusual super-
51 ring structure and global aromaticity. *Chem* **2018**, *4*, 1586–1595.
52
53
54
55
56 [56] Casanova, D.; Head-Gordon, M. Restricted active space spin-flip con-
57
58
59
60

- figuration interaction approach: theory, implementation and examples. *Physical Chemistry Chemical Physics* **2009**, *11*, 9779–9790.
- [57] Lin, C.-Y.; Hui, K.; Chung, J.-H.; Chai, J.-D. Self-Consistent Determination of the Fictitious Temperature in Thermally-Assisted-Occupation Density Functional Theory. *RSC Advances* **2017**, *7*, 50496–50507.
- [58] Grimme, S.; Hansen, A. A practicable real-space measure and visualization of static electron-correlation effects. *Angewandte Chemie International Edition* **2015**, *54*, 12308–12313.
- [59] Bauer, C. A.; Hansen, A.; Grimme, S. The fractional occupation number weighted density as a versatile analysis tool for molecules with a complicated electronic structure. *Chemistry-A European Journal* **2017**, *23*, 6150–6164.
- [60] Head-Gordon, M. Characterizing unpaired electrons from the one-particle density matrix. *Chemical Physics Letters* **2003**, *372*, 508–511.
- [61] Yeh, C.-N.; Chai, J.-D. Role of Kekulé and non-Kekulé structures in the radical character of alternant polycyclic aromatic hydrocarbons: a TAO-DFT study. *Scientific Reports* **2016**, *6*, 30562.
- [62] Nakano, M.; Kishi, R.; Ohta, S.; Takahashi, H.; Kubo, T.; Kamada, K.; Ohta, K.; Botek, E.; Champagne, B. Relationship between third-order nonlinear optical properties and magnetic interactions in open-shell systems: a new paradigm for nonlinear optics. *Physical Review Letters* **2007**, *99*, 033001.
- [63] Pérez-Guardiola, A.; Sandoval-Salinas, M. E.; Casanova, D.; San-Fabián, E.; Pérez-Jiménez, A.; Sancho-García, J.-C. The role of topol-

- 1
2
3
4
5
6
7
8
9
10
11
12
13
14
15
16
17
18
19
20
21
22
23
24
25
26
27
28
29
30
31
32
33
34
35
36
37
38
39
40
41
42
43
44
45
46
47
48
49
50
51
52
53
54
55
56
57
58
59
60
- ogy in organic molecules: origin and comparison of the radical character in linear and cyclic oligoacenes and related oligomers. *Physical Chemistry Chemical Physics* **2018**, *20*, 7112–7124.
- [64] Yamaguchi, K.; Fukui, H.; Fueno, T. Molecular orbital (MO) theory for magnetically interacting organic compounds. Ab-initio MO calculations of the effective exchange integrals for cyclophane-type carbene dimers. *Chemistry Letters* **1986**, *15*, 625–628.
- [65] Yamaguchi, K.; Takahara, Y.; Fueno, T.; Houk, K. N. Extended Hartree-Fock (EHF) theory of chemical reactions. *Theoretica Chimica Acta* **1988**, *73*, 337–364.
- [66] Yamanaka, S.; Okumura, M.; Nakano, M.; Yamaguchi, K. EHF theory of chemical reactions Part 4. UNO CASSCF, UNO CASPT2 and R(U)HF coupled-cluster (CC) wavefunctions. *Journal of Molecular Structure: THEOCHEM* **1994**, *310*, 205–218.
- [67] Rinkevicius, Z.; Vahtras, O.; Ågren, H. Spin-flip time dependent density functional theory applied to excited states with single, double, or mixed electron excitation character. *The Journal of Chemical Physics* **2010**, *133*, 114104.
- [68] Canola, S.; Casado, J.; Negri, F. The double exciton state of conjugated chromophores with strong diradical character: insights from TDDFT calculations. *Physical Chemistry Chemical Physics* **2018**, *20*, 24227–24238.
- [69] Canola, S.; Dai, Y.; Negri, F. The Low Lying Double-Exciton State of Conjugated Diradicals: Assessment of TDUDFT and Spin-Flip TDDFT Predictions. *Computation* **2019**, *7*, 68.

- 1
2
3
4
5
6
7
8 [70] Krylov, A. I. Spin-flip configuration interaction: an electronic struc-
9 ture model that is both variational and size-consistent. *Chemical*
10 *Physics Letters* **2001**, *350*, 522–530.
11
12
13
14 [71] Krylov, A. I. Spin-flip equation-of-motion coupled-cluster electronic
15 structure method for a description of excited states, bond breaking,
16 diradicals, and triradicals. *Accounts of Chemical Research* **2006**, *39*,
17 83–91.
18
19
20
21
22 [72] Casanova, D.; Krylov, A. I. *Physical Chemistry Chemical Physics*,
23 2020,, DOI: 10.1039/C9CP06507E.
24
25
26 [73] Tao, J.; Perdew, J. P.; Staroverov, V. N.; Scuseria, G. E. Climbing
27 the density functional ladder: Nonempirical meta-generalized gradi-
28 ent approximation designed for molecules and solids. *Physical Review*
29 *Letters* **2003**, *91*, 146401.
30
31
32
33
34 [74] Staroverov, V. N.; Scuseria, G. E.; Tao, J.; Perdew, J. P. Comparative
35 assessment of a new nonempirical density functional: Molecules and
36 hydrogen-bonded complexes. *The Journal of Chemical Physics* **2003**,
37 *119*, 12129–12137.
38
39
40
41
42 [75] Weigend, F.; Ahlrichs, R. Balanced basis sets of split valence, triple
43 zeta valence and quadruple zeta valence quality for H to Rn: De-
44 sign and assessment of accuracy. *Physical Chemistry Chemical Physics*
45 **2005**, *7*, 3297–3305.
46
47
48
49
50 [76] Kossmann, S.; Neese, F. Comparison of two efficient approximate
51 Hartee–Fock approaches. *Chemical Physics Letters* **2009**, *481*, 240–
52 243.
53
54
55
56
57
58
59
60

- 1
2
3
4
5
6
7
8 [77] Weigend, F. Hartree–Fock exchange fitting basis sets for H to Rn.
9 *Journal of Computational Chemistry* **2008**, *29*, 167–175.
10
11
12 [78] Pettersen, E. F.; Goddard, T. D.; Huang, C. C.; Couch, G. S.; Green-
13 blatt, D. M.; Meng, E. C.; Ferrin, T. E. UCSF Chimera: A Visu-
14 alization System for Exploratory Research and Analysis. *Journal of*
15 *Computational Chemistry* **2004**, *25*, 1605–1612.
16
17
18 [79] Neese, F. Software update: the ORCA program system, version 4.0.
19 *Wiley Interdisciplinary Reviews: Computational Molecular Science*
20 **2018**, *8*, e1327.
21
22
23
24
25
26 [80] Schmidt, M. W.; Baldridge, K. K.; Boatz, J. A.; Elbert, S. T.; Gor-
27 don, M. S.; Jensen, J. H.; Koseki, S.; Matsunaga, N.; Nguyen, K. A.;
28 Su et al., S. General atomic and molecular electronic structure system.
29 *Journal of Computational Chemistry* **1993**, *14*, 1347–1363.
30
31
32
33
34 [81] Becke, A. D. A new mixing of Hartree–Fock and local density-
35 functional theories. *The Journal of Chemical Physics* **1993**, *98*, 1372–
36 1377.
37
38
39
40 [82] Orms, N.; Krylov, A. I. Singlet–triplet energy gaps and the degree
41 of diradical character in binuclear copper molecular magnets char-
42 acterized by spin-flip density functional theory. *Physical Chemistry*
43 *Chemical Physics* **2018**, *20*, 13127–13144.
44
45
46
47 [83] Bernard, Y. A.; Shao, Y.; Krylov, A. I. General formulation of spin-flip
48 time-dependent density functional theory using non-collinear kernels:
49 Theory, implementation, and benchmarks. *The Journal of Chemical*
50 *Physics* **2012**, *136*, 204103.
51
52
53
54 [84] Shao et al., Y. Advances in molecular quantum chemistry contained in
55
56
57
58
59
60

- 1
2
3
4
5
6
7
8 the Q-Chem 4 program package. *Molecular Physics* **2015**, *113*, 184–
9 215.
- 10
11
12 [85] Chai, J.-D.; Head-Gordon, M. Long-range corrected hybrid density
13 functionals with damped atom–atom dispersion corrections. *Physical*
14 *Chemistry Chemical Physics* **2008**, *10*, 6615–6620.
- 15
16
17 [86] Schindler, M.; Kutzelnigg, W. Theory of magnetic susceptibilities and
18 NMR chemical shifts in terms of localized quantities. II. Application
19 to some simple molecules. *The Journal of Chemical Physics* **1982**, *76*,
20 1919–1933.
- 21
22
23 [87] Jensen, F. Basis set convergence of nuclear magnetic shielding con-
24 stants calculated by density functional methods. *Journal of Chemical*
25 *Theory and Computation* **2008**, *4*, 719–727.
- 26
27
28 [88] Stoychev, G. L.; Auer, A. A.; Neese, F. Automatic generation of aux-
29 iliary basis sets. *Journal of Chemical Theory and Computation* **2017**,
30 *13*, 554–562.
- 31
32
33 [89] Neese, F. Calculation of the zero-field splitting tensor on the basis
34 of hybrid density functional and Hartree-Fock theory. *The Journal of*
35 *Chemical Physics* **2007**, *127*, 164112.
- 36
37
38 [90] Jost, P.; van Wüllen, C. Why spin contamination is a major problem
39 in the calculation of spin–spin coupling in triplet biradicals. *Physical*
40 *Chemistry Chemical Physics* **2013**, *15*, 16426–16427.
- 41
42
43 [91] Pérez-Guardiola, A.; Ortiz-Cano, R.; Sandoval-Salinas, M. E.;
44 Fernández-Rossier, J.; Casanova, D.; Pérez-Jiménez, A.; Sancho-
45 Garcia, J.-C. From cyclic nanorings to single-walled carbon nanotubes:
46 disclosing the evolution of their electronic structure with the help of
47
48
49
50
51
52
53
54
55
56
57
58
59
60

- 1
2
3
4
5
6
7
8 theoretical methods. *Physical Chemistry Chemical Physics* **2019**, *21*,
9 2547–2557.
10
11
12 [92] Swart, M.; Gruden, M. Spinning around in transition-metal chemistry.
13 *Accounts of Chemical Research* **2016**, *49*, 2690–2697.
14
15
16 [93] Song, S.; Kim, M.-C.; Sim, E.; Benali, A.; Heinonen, O.; Burke, K.
17 Benchmarks and reliable DFT results for spin gaps of small ligand Fe
18 (II) complexes. *Journal of Chemical Theory and Computation* **2018**,
19 *14*, 2304–2311.
20
21
22 [94] Rousseau, L.; Brémond, E.; Lefèvre, G. Assessment of the ground spin
23 state of iron (I) complexes: insights from DFT predictive models. *New*
24 *Journal of Chemistry* **2018**, *42*, 7612–7616.
25
26
27 [95] Richert, S.; Tait, C. E.; Timmel, C. R. Delocalisation of photoexcited
28 triplet states probed by transient EPR and hyperfine spectroscopy.
29 *Journal of Magnetic Resonance* **2017**, *280*, 103–116.
30
31
32 [96] Buta, M. C.; Toader, A. M.; Frecus, B.; Oprea, C. I.; Cimpoesu, F.;
33 Ionita, G. Molecular and Supramolecular Interactions in Systems with
34 Nitroxide-Based Radicals. *International Journal of Molecular Sciences*
35 **2019**, *20*, 4733.
36
37
38 [97] Tawada, Y.; Tsuneda, T.; Yanagisawa, S.; Yanai, T.; Hirao, K. A
39 long-range-corrected time-dependent density functional theory. *The*
40 *Journal of Chemical Physics* **2004**, *120*, 8425–8433.
41
42
43 [98] Sinnecker, S.; Neese, F. Spin-Spin Contributions to the Zero-Field
44 Splitting Tensor in Organic Triplets, Carbenes and Biradicals A Den-
45 sity Functional and Ab Initio Study. *The Journal of Physical Chem-*
46 *istry A* **2006**, *110*, 12267–12275.
47
48
49
50
51
52
53
54
55
56
57
58
59
60

- 1
2
3
4
5
6
7
8 [99] Perumal, S. S. Zero-field splitting of compact trimethylenemethane
9 analogue radicals with density functional theory. *Chemical Physics*
10 *Letters* **2011**, *501*, 608–611.
11
12
13
14 [100] Ye, S.; Neese, F. How do heavier halide ligands affect the signs and
15 magnitudes of the zero-field splittings in halogenonickel (II) scorpione
16 complexes? A theoretical investigation coupled to ligand-field
17 analysis. *Journal of Chemical Theory and Computation* **2012**, *8*, 2344–
18 2351.
19
20
21
22
23
24 [101] Yanai, T.; Tew, D. P.; Handy, N. C. A new hybrid exchange–
25 correlation functional using the Coulomb-attenuating method (CAM-
26 B3LYP). *Chemical Physics Letters* **2004**, *393*, 51–57.
27
28
29
30 [102] Duboc, C.; Ganyushin, D.; Sivalingam, K.; Collomb, M.-N.; Neese, F.
31 Systematic theoretical study of the zero-field splitting in coordination
32 complexes of Mn (III). Density functional theory versus multireference
33 wave function approaches. *The Journal of Physical Chemistry A* **2010**,
34 *114*, 10750–10758.
35
36
37
38
39
40 [103] Ganyushin, D.; Gilka, N.; Taylor, P. R.; Marian, C. M.; Neese, F.
41 The resolution of the identity approximation for calculations of spin-
42 spin contribution to zero-field splitting parameters. *The Journal of*
43 *Chemical Physics* **2010**, *132*, 144111.
44
45
46
47
48 [104] Inoue, J.; Fukui, K.; Kubo, T.; Nakazawa, S.; Sato, K.; Shiomi, D.;
49 Morita, Y.; Yamamoto, K.; Takui, T.; Nakasuji, K. The first detection
50 of a Clar’s hydrocarbon, 2,6,10-tri-tert-butyltriangulene: a ground-
51 state triplet of non-Kekulé polynuclear benzenoid hydrocarbon. *Jour-*
52 *nal of the American Chemical Society* **2001**, *123*, 12702–12703.
53
54
55
56
57
58
59
60

- 1
2
3
4
5
6
7
8 [105] Bayliss, S. L.; Chepelianskii, A. D.; Sepe, A.; Walker, B. J.; Ehrler, B.;
9 Bruzek, M. J.; Anthony, J. E.; Greenham, N. C. Geminate and
10 nongeminate recombination of triplet excitons formed by singlet fis-
11 sion. *Physical Review Letters* **2014**, *112*, 238701.
12
13
14
15 [106] Pershin, A.; Hall, D.; Lemaire, V.; Sancho-Garcia, J.-C.; Muccioli, L.;
16 Zysman-Colman, E.; Beljonne, D.; Olivier, Y. Highly emissive excitons
17 with reduced exchange energy in thermally activated delayed fluores-
18 cent molecules. *Nature Communications* **2019**, *10*, 597.
19
20
21
22
23
24
25
26
27
28
29
30
31
32
33
34
35
36
37
38
39
40
41
42
43
44
45
46
47
48
49
50
51
52
53
54
55
56
57
58
59
60

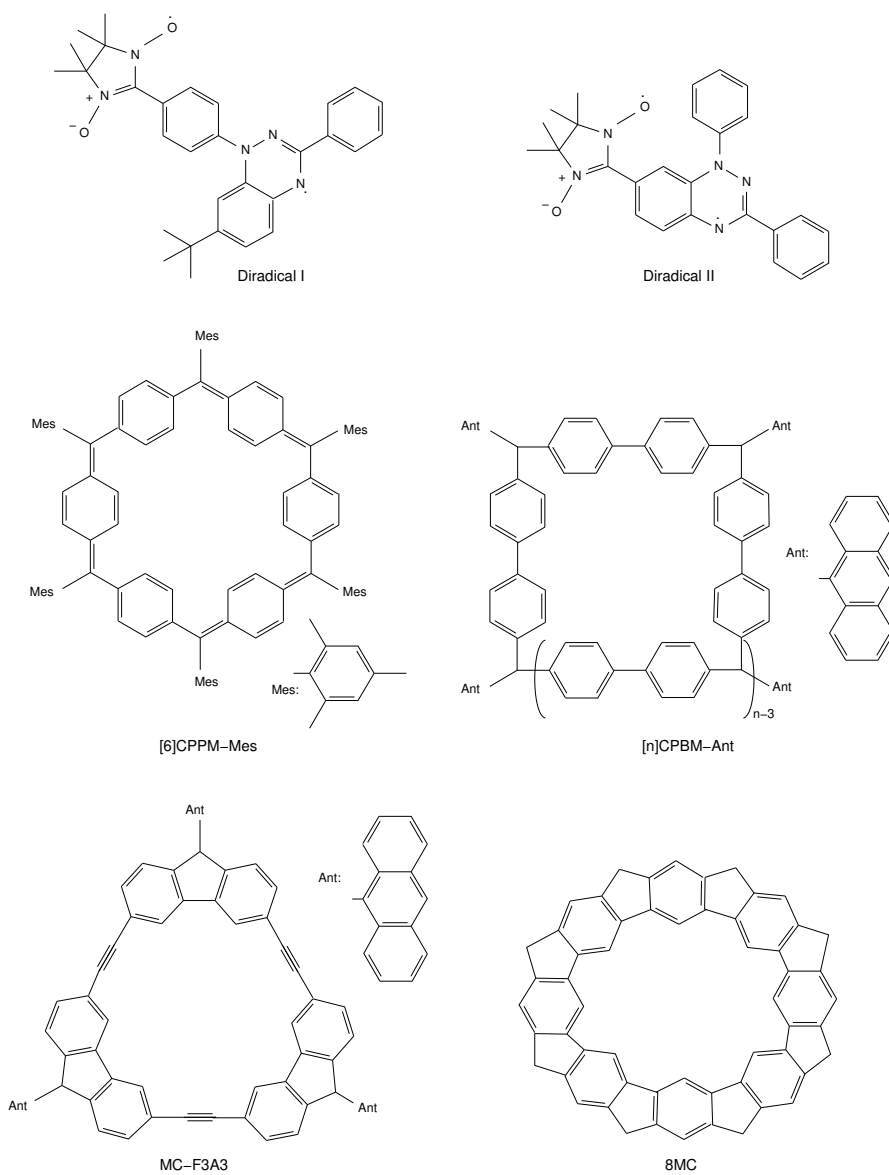


Figure 1: Chemical structures of the investigated compounds

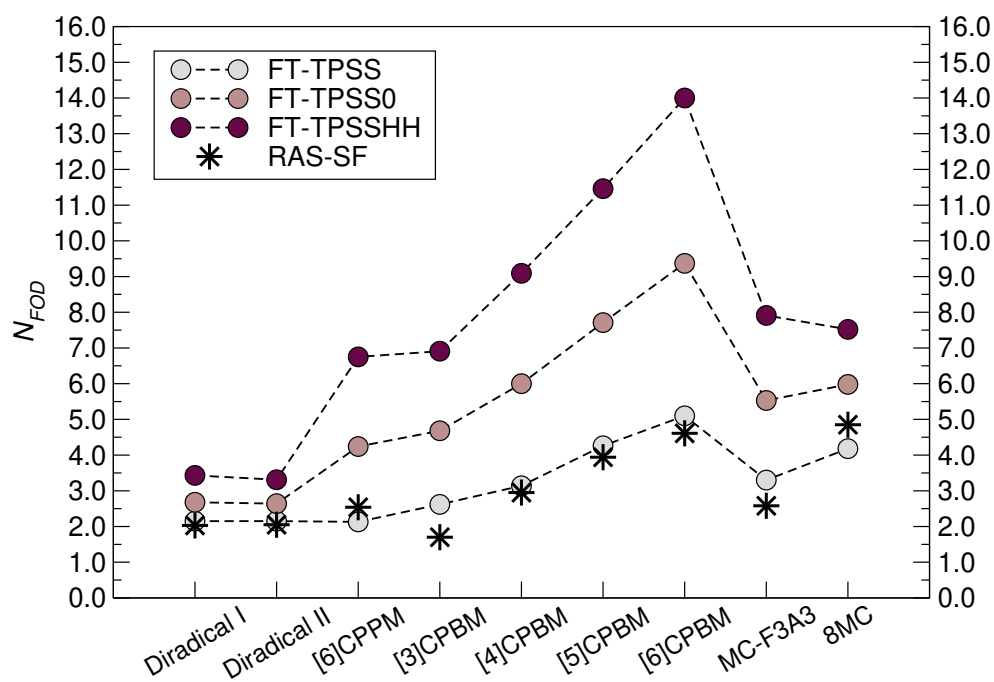


Figure 2: Comparison between FT-DFT and RAS-SF N_{FOD} values for the low-spin state of the set of studied compounds.

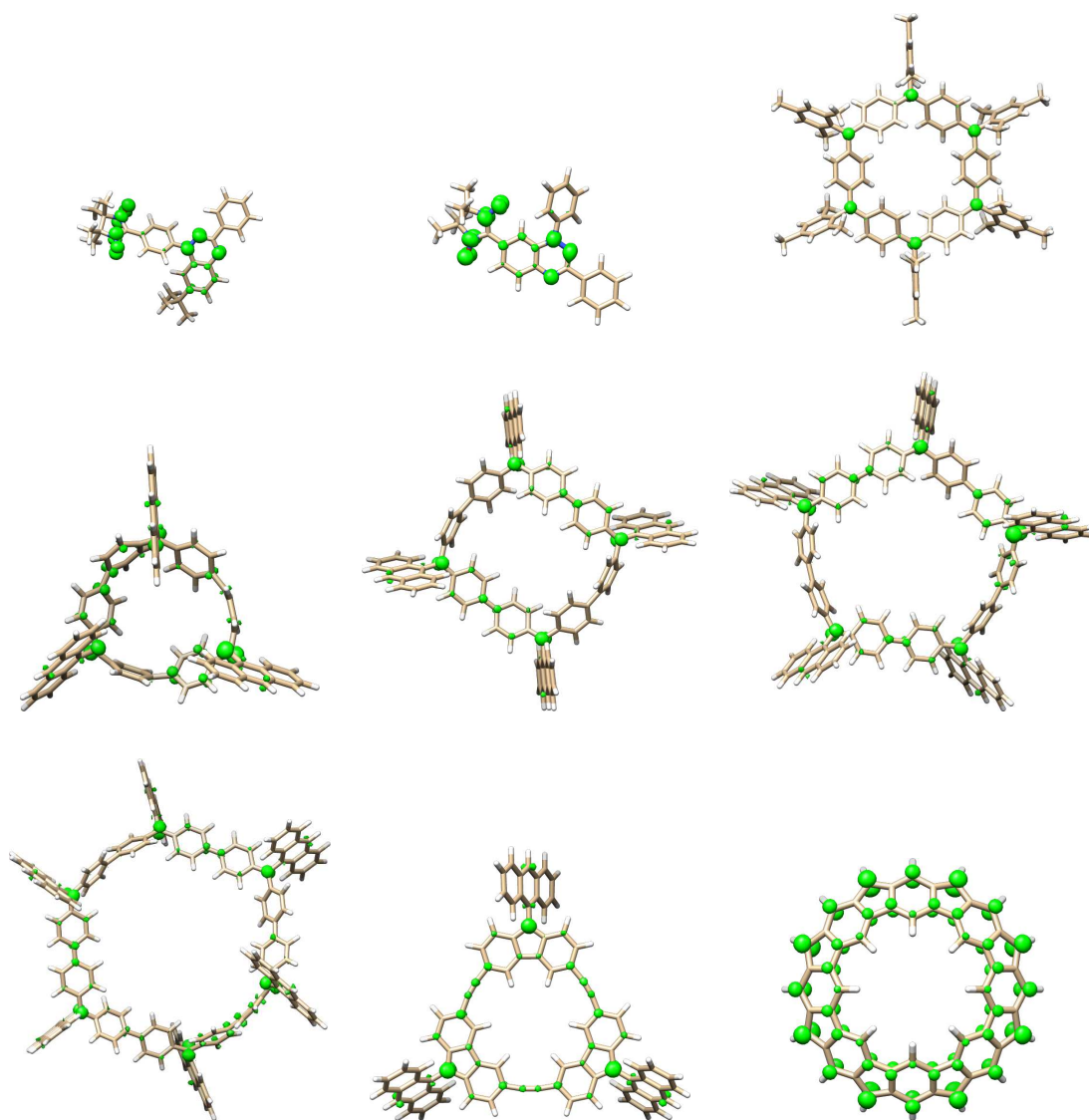


Figure 3: FOD density plots ($\sigma = 0.005 \text{ e/bohr}^3$) obtained from the FT-TPSS/def2-TZVP method for the set of studied compounds.

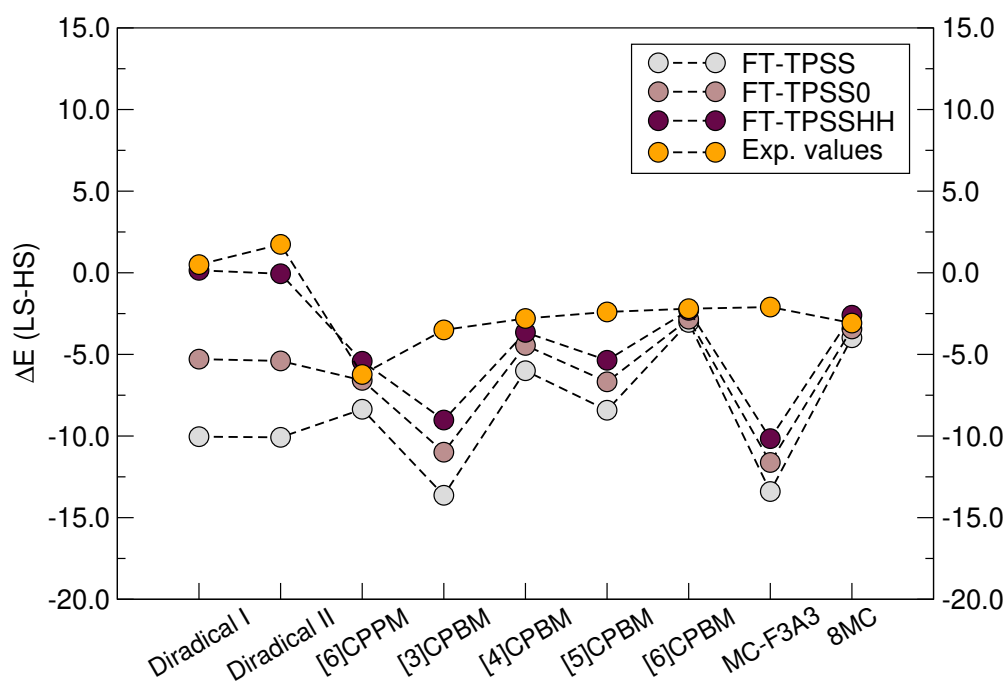


Figure 4: Comparison between $\Delta E(\text{LS} - \text{HS})$ (kcal/mol) computed (FT-DFT) and experimental values for the set of studied compounds.

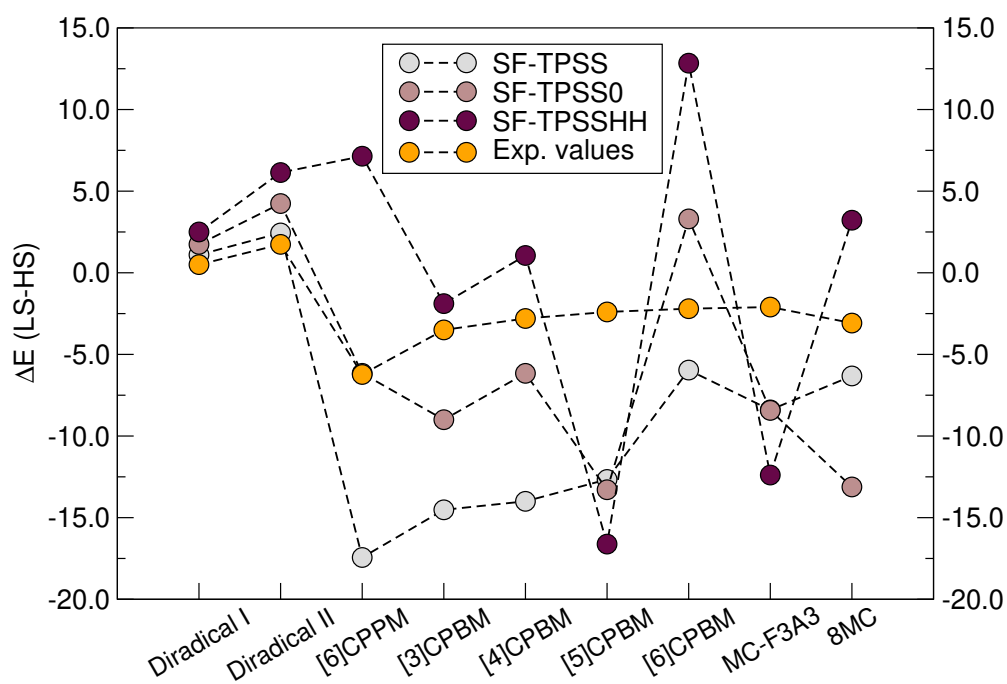


Figure 5: Comparison between $\Delta E(\text{LS} - \text{HS})$ (kcal/mol) computed (SF-DFT) and experimental values for the set of studied compounds.

Table 1: N_{FOD} values obtained at different theoretical levels.

Compound	GS	FT-TPSS		FT-TPSS0		FT-TPSSH	
		$N_{FOD}(\text{LS})$	$N_{FOD}(\text{HS})$	$N_{FOD}(\text{LS})$	$N_{FOD}(\text{HS})$	$N_{FOD}(\text{LS})$	$N_{FOD}(\text{HS})$
Diradical I ^a	T ₀	2.15	0.81	2.68	1.44	3.43	2.23
Diradical II ^a	T ₀	2.15	0.79	2.64	1.42	3.31	2.10
[6]CPPM-Mes	S ₀	2.13	2.90	4.24	4.82	6.75	7.24
[3]CPBM-Ant	D ₀	2.62	2.78	4.68	4.78	6.91	6.99
[4]CPBM-Ant	S ₀	3.14	3.70	6.00	6.43	9.09	9.44
[5]CPBM-Ant	D ₀	4.26	4.61	7.71	7.95	11.46	11.66
[6]CPBM-Ant	S ₀	5.10	5.50	9.37	9.63	14.00	14.17
MC-F3A3	D ₀	3.30	3.13	5.53	5.37	7.91	7.73
8MC	S ₀	4.18	4.34	5.98	5.93	7.52	7.36

^a Note that for these systems the header classification do not apply, since the ground-state is already the T₀ and thus the HS state.

Table 2: Calculated radical indices^a (y_i^α) by the FT-DFT method at the TPSS/def2-TZVP level.

Compound	y_0^α	y_1^α	y_2^α	y_3^α
Diradical I	0.49	0.03	0.02	0.00
Diradical II	0.49	0.03	0.00	0.00
[6]CPPM-Mes	0.24	0.22	0.04	0.00
[3]CPBM-Ant	0.35	0.08	0.08	0.08
[4]CPBM-Ant	0.28	0.21	0.06	0.06
[5]CPBM-Ant	0.31	0.29	0.08	0.08
[6]CPBM-Ant	0.34	0.28	0.21	0.06
MC-F3A3	0.46	0.07	0.07	0.06
8MC	0.30	0.30	0.21	0.21

^a Note that $y_i^\alpha = y_i^\beta$.

Table 3: Energy difference (kcal/mol) between the low-spin (LS) and high-spin (HS) states, $\Delta E(\text{LS} - \text{HS})$, obtained at the FT-DFT level.

Compound	GS	FT-TPSS	FT-TPSS0	FT-TPSSHH	Exp.
Diradical I	T ₀	-10.04	-5.29	0.15	0.50±0.02
Diradical II	T ₀	-10.08	-5.40	-0.06	1.74±0.07
[6]CPPM-Mes	S ₀	-8.36	-6.50	-5.42	-6.23±0.78
[3]CPBM-Ant	D ₀	-13.63	-10.99	-9.02	-3.5
[4]CPBM-Ant	S ₀	-6.00	-4.45	-3.65	-2.8
[5]CPBM-Ant	D ₀	-8.42	-6.68	-5.36	-2.4
[6]CPBM-Ant	S ₀	-3.54	-2.84	-2.30	-2.2
MC-F3A3	D ₀	-13.40	-11.62	-10.16	-2.10
8MC	S ₀	-3.98	-3.44	-2.60	-3.08
	MSE	-6.4	-4.1	-2.0	
	MUE	6.4	4.1	2.3	
	MIN	0.9	0.4	0.4	
	MAX	11.8	9.5	8.1	

Table 4: Energy difference (kcal/mol) between the Broken-Symmetry (BS) and high-spin (HS) states, $\Delta E(\text{BS} - \text{HS})$, and the corresponding $\Delta E(\text{LS} - \text{HS})$ corrected, obtained at the SF-DFT level.

Compound	GS	SF-TPSS		SF-TPSS0		SF-TPSSHH		Exp.
		$\Delta E(\text{BS} - \text{HS})$	$\Delta E(\text{LS} - \text{HS})$	$\Delta E(\text{BS} - \text{HS})$	$\Delta E(\text{LS} - \text{HS})$	$\Delta E(\text{BS} - \text{HS})$	$\Delta E(\text{LS} - \text{HS})$	
Diradical I	T ₀	0.55	1.10	0.88	1.74	1.32	2.50	0.50±0.02
Diradical II	T ₀	1.23	2.44	2.18	4.24	3.34	6.14	1.74±0.07
[6]CPPM-Mes	S ₀	-18.44	-17.44	-8.61	-6.16	12.94	7.14	-6.23±0.78
[3]CPBM-Ant	D ₀	-14.61	-14.52	-9.21	-9.00	-2.05	-1.89	-3.5
[4]CPBM-Ant	S ₀	-14.07	-14.00	-8.62	-6.16	1.27	1.06	-2.8
[5]CPBM-Ant	D ₀	-12.60	-12.66	-10.16	-13.29	-11.41	-16.62	-2.4
[6]CPBM-Ant	S ₀	-6.29	-5.96	3.48	3.30	15.85	12.84	-2.2
MC-F3A3	D ₀	-7.89	-8.40	-5.97	-8.43	-7.47	-12.39	-2.10
8MC	S ₀	-6.72	-6.32	-8.06	-13.12	1.93	3.22	-3.08
	MSE	-6.5	-6.2	-2.7	-3.0	4.0	2.4	
	MUE	6.5	6.5	4.1	5.0	7.2	7.9	
	MIN	0.0	0.6	0.4	0.1	0.8	1.6	
	MAX	12.2	11.2	7.8	10.9	19.2	15.0	

43

Table 5: Energy difference (kcal/mol) between the low-spin (LS) and high-spin (HS) states, $\Delta E(\text{LS} - \text{HS})$, obtained at the SF-TDDFT level.

Compound	GS	SF-TDBHLYP	Exp.
Diradical I	T ₀	-9.34	0.50±0.02
Diradical II	T ₀	-9.94	1.74±0.07
[6]CPPM-Mes	S ₀	-3.37	-6.23±0.78
[3]CPBM-Ant	D ₀	-17.99	-3.5
[4]CPBM-Ant	S ₀	-17.80	-2.8
[5]CPBM-Ant	D ₀	-15.86	-2.4
[6]CPBM-Ant	S ₀	-9.34	-2.2
MC-F3A3	D ₀	-6.69	-2.10
8MC	S ₀	-0.57	-3.08
	MSE	-7.9	
	MUE	9.1	
	MIN	2.5	
	MAX	15.0	

Table 6: Calculated D and E EPR parameters (D/hc and E/hc in 10^3cm^{-1}) and exciton size (Δr , in \AA) at the $\omega\text{B97X-D/IGLO-II}$ level, of the lowest triplet state of the selected compounds.

Compound	D	E	Δr
Diradical I	-5.52	-0.80	7.8
Diradical II	-11.13	-3.66	6.2
[6]CPPM-Mes	-12.60	-0.56	5.9
[4]CPBM-Ant	-13.04	-1.74	5.8
[6]CPBM-Ant	-10.05	-0.04	6.4
8MC	4.29	0.00	8.5

1
2
3
4
5
6
7
8
9
10
11
12
13
14
15
16
17
18
19
20
21
22
23
24
25
26
27
28
29
30
31
32
33
34
35
36
37
38
39
40
41
42
43
44
45
46
47
48
49
50
51
52
53
54
55
56
57
58
59
60

FT-DFT / SF-DFT / SF-TDDFT / RAS-SF

